PHYSICAL REVIEW E VOLUME 58, NUMBER 2 AUGUST 1998

Topological effects on statics and dynamics of knotted polymers

Yu-Jane Sheng,[1] Pik-Yin Lai,[1,*] and Heng-Kwong Tsao[2]
[1]Department of Physics and Center for Complex Systems, National Central University, Chung-li, Taiwan 320, Republic of China
[2]Department of Chemical Engineering, National Central University, Chung-li, Taiwan 320, Republic of China

(Received 6 November 1997)

Using dynamic Monte Carlo simulations, our results on the radii of gyration of knot polymers suggest that prime and two-factor composite knots belong to different groups. From the studies of nonequilibrium relaxation dynamics on cut prime knots, we find that even prime knots should be classified into different groups, such as $(3_1,5_1,\ldots)$, $(4_1,6_1,\ldots)$, and $(5_2,7_2,\ldots)$, etc., based on their topological similarity and their polynomial invariants. By scaling calculations, the nonequilibrium relaxation time is found to increase roughly as $p^{12/5}$, where p is the topological invariant length-to-diameter ratio of the knot at its maximum inflated state. This prediction is further confirmed by our data. [S1063-651X(98)50408-4]

PACS number(s): 61.41.+e, 83.10.Nn, 87.10.+e

The topological effects of knots play crucial roles in many molecular biological phenomena. It is known that there are certain types of enzymes [1–3] that act on circular DNA's and produce different types of DNA knots. It would be of great importance to study those nonequilibrium dynamical transformation processes for further understanding the fundamentals of animate nature. Studies of the knotted polymer systems are limited, despite the great advances that have been made in classifying knots and topological invariants [4–7]. Up until now, most studies have concentrated on relating the topological invariants of knots to the static properties of the knotted polymers. Quake developed a phenomenological model [8] of the effects of knot complexity on the static and dynamic properties in terms of the number of essential crossings C. The theory has been tested against computer simulations and was in good agreement with the result on the average radius of gyration. Attempts to find topological effects on the dynamic properties of knotted polymers are rare [8]. Topological constraints are especially important in most dynamic phenomena proceeding in systems of entangled polymer coils or knotted ring polymers. The prohibition against chain crossing in a system restricts the number of its possible conformations to one topological type. The only conformations are those that are topologically equivalent to one another. These conformations can only appear or disappear via continuous chain deformations. The fact that ring polymers possess topological memory is expected to hinder their relaxation motions. In this study, Monte Carlo simulations are performed to study the nonequilibrium dynamic relaxation processes of knotted polymers. Experiments had shown [1,3] that a certain link in some ring DNA breaks up upon the action of enzymes (such as topoisomerase) and reconnects again after the switching of interlinked strands, resulting in a knot structure. The relaxation dynamics of the knotted polymer is therefore important in such a process. If the relaxation time is too fast, the knot will untie itself before the link reconnects again and no knot structure will result. Since there is neither experimental observations nor theoretical models that would allow the relaxation dynamics of cut ring knotted polymers to be predicted, our simulation results should be helpful in the study of ring polymer topology. The results can be used to formulate theoretical models or to be compared with experiments. For the dynamics, we investigate a ring polymer with a certain topological complexity that is initially well equilibrated and then cut at a randomly picked link. The relaxation processes are monitored and analyzed. Our results suggest a possible classification of the relaxation properties of knotted polymers in terms of their similarities on local topology and polynomial invariants.

The polymer chain studied in the simulation is modeled as beads connected by stiff springs. The interactions between the nonbonded beads are through the square-well potential

$$U_{nb}=\begin{cases}\infty & (r<\sigma)\\ -\varepsilon & (\sigma\leqslant r<\lambda\sigma)\\ 0 & (\lambda\sigma\leqslant r),\end{cases} \tag{1}$$

where ε and σ are the energy and size parameters, respectively, and $\lambda=1.5$. The monomeric ε and σ are units used for the reduced quantities for temperature ($T^*=k_BT/\varepsilon$) and distances. The interactions between bonded beads are represented by a cut-off harmonic spring potential as

$$U_b=\frac{1}{2}k\sigma^2\left(\frac{r}{\sigma}-1.2\right)^2,\quad 1.0<\frac{r}{\sigma}\leqslant 1.4. \tag{2}$$

The potential is infinite elsewhere. We have chosen $k\sigma^2/\varepsilon=400$. The parameters in the model are chosen to forbid any bond crossing to occur within the knotted chain. We have studied the knotted polymers up to nine crossings: 3_1, 4_1, 5_1, 5_2, 6_1, 6_2, 6_3, 7_1, 7_2, 8_1, 9_1, and some composite knots. The standard notation [7] for uniquely labeling a knot is C_K, where C is the number of essential crossings and K is an index for a particular knot. Figure 1 displays some of the knot types studied in this work. $T^*=10$ is chosen so that the system is in the good solvent regime and the Flory value of $\nu=3/5$ is used throughout here. The initial configurations are generated by growing the chain bead by bead to the desired

---

[*] Author to whom correspondence should be addressed. Electronic address: pylai@spl1.phy.ncu.edu.tw

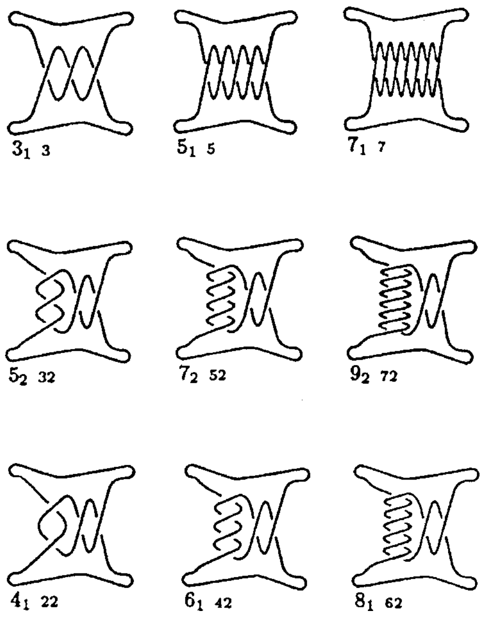

FIG. 1. Schematic knot diagrams. The $(3_1, 5_1, \ldots)$, $(4_1, 6_1, \ldots)$, and the $(5_2, 7_2, \ldots)$ groups. The Conway notations of the knots are also shown.

length and knot type. The trial moves employed for chains are bead displacement motions [9] that involve randomly picking a bead and displacing it to a new position in the vicinity of the old position. The new configurations resulting from this move are accepted according to the standard Metropolis acceptance criterion [10]. All runs are equilibrated for several million steps. Measurements for static properties such as mean radius of gyration are taken over a period of $10^6 - 4 \times 10^6$ Monte Carlo steps (MCS) per monomer. The knotted ring polymer is allowed to equilibrate for a long time before it is cut randomly at one bond at $t=0$. The nonequilibrium relaxation process is characterized by the time dependence of the radius of gyration $R_g(t)$ as it approaches its long time limit. Averages over different realizations (typically ~ 300 to 500) of the relaxation processes are performed. Time is measured in units of Monte Carlo steps per monomer.

Quake used the number of crossings (C) to measure the knot complexity and obtained the scaling law for the radius of gyration as $R_g \propto N^{\nu} C^{1/3-\nu}$, which was verified by Monte Carlo simulations. However, C is a fairly weak topological invariant. As we know there are seven knots with seven crossings and 166 knots with 10 crossings. The number of knots increases rapidly with the number of crossings. Grosberg *et al.* [11] introduced a topological invariant p that is the aspect ratio of the length (L) to the diameter (d) of a knotted polymer at its maximum inflated state, $p = L/d$. The more complicated the knot, the greater the value p. According to the calculations of Katritch *et al.* [12], the knot 6_1 $(p=29.3)$ is less complex than 6_3 $(p=30.5)$ and the knot 8_1 $(p=37)$ is more complex than 8_{19} $(p=31)$. p distinguishes rather well between different knot types and thus is a better topological invariant than C. Grosberg *et al.* used the classic Flory approach to estimate the equilibrium polymer size by balancing the rubberlike elasticity and volume interactions between monomers, and found that [11] $R_g \sim N^{\nu} p^{-4/15}$ in the good solvent regime. We have performed simulations to check this relation and the results are shown in Fig. 2. Two groups of knots are observed from our data. One group contains the prime knots $(3_1, 4_1, 5_1, 5_2, 6_1, 6_2, 6_3, 7_1, 7_2, 8_1, 9_1)$ and the other group consists of the composite knots: $3_1\#3_1$ (granny), $3_1\#-3_1$ (square), $3_1\#4_1$, and $3_1\#5_1$. Both of the groups show rather good linear relations with slopes relatively close to $-4/15$. However, the values of the radius of gyration for the composite knots are systematically larger than the prime knots for $N=60$ and 82. This indicates that the static properties are not only determined entirely by the topological invariant p. The $\langle R_g \rangle$ of the three-factor composite knot $3_1\#3_1\#3_1 (N=82)$ is also calculated, which shows an obvious deviation from the group $(3_1\#3_1, 3_1\#4_1, 3_1\#5_1)$. This further suggests that a different number of factors in the composite knots may result in different groups. Recently, Katritch *et al.* [13] found that there exists an exact additivity of the writhe number, but subadditivity (different degrees of deficits for a different number of factors) of p for composite knots. Thus, it is plausible to assume that different groups of knots exist. On the other hand, our data for both prime and composite knots obey $R_g \sim N^{\nu}$, suggesting that this scaling is universal [14]. However, it is noted that, as p increases, deviation from $R_g \sim N^{\nu} p^{-4/15}$ becomes significant. This is because the polymer is crossing over to the maximal tightened knot regime. In this regime, the polymer coils up so tightly, almost as a compact ball, and R_g becomes independent of p and solvent quality; $R_g \sim N^{1/3}$. The uniqueness of this regime is caused by the strong constraint imposed on the knotted ring conformation.

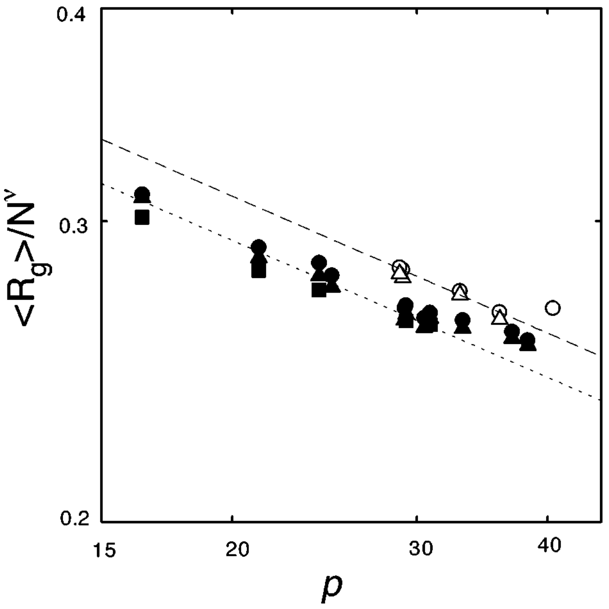

FIG. 2. Average radius of gyration vs the aspect ratio (p) for knots of various chain lengths. Dotted lines denote slopes of $-4/15$. Filled symbols represent the prime knots $3_1, 4_1, 5_1, \ldots 9_1$: ■, $N=42$; ▲, $N=60$; ●, $N=82$. Open symbols are composite knots: △, $N=60$; ○, $N=82$. For increasing values of p: ■, 3_1, 4_1, 5_1, 6_1, 6_3; ▲, 3_1, 4_1, 5_1, 5_2, 6_2, 6_1, 6_3, 7_1, 7_2, 8_1, 9_1; ●, 3_1, 4_1, 5_1, 5_2, 6_2, 6_1, 6_3, 7_1, 7_2, 8_1, 9_1; △, $3_1\#-3_1$, $3_1\#3_1$, $3_1\#4_1$, $3_1\#5_1$; ○, $3_1\#-3_1$, $3_1\#3_1$, $3_1\#4_1$, $3_1\#5_1$, $3_1\#3_1\#3_1$.

As for the studies of nonequilibrium dynamics, we focus only on prime knots. The knotted ring polymer is cut at a randomly picked link at $t=0$ and the chain starts to relax

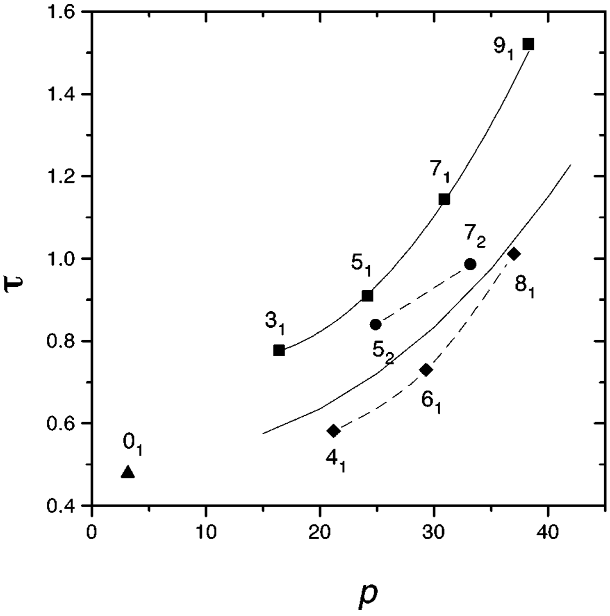

FIG. 3. Monte Carlo data for the nonequilibrium relaxation time (in units of 10^5 MCS/monomer) vs p for $N=60$. Solid curves are $\tau\sim p^{12/5}$. The lower solid curve is just a guide for the eyes.

TABLE I. Table for the different knot groups in this paper with their Alexander polynomials $\Delta(t)$ and Conway notations. C is the number of crossings in the knot. t is just an algebraic variable.

Knot group	Alexander polynomial $\Delta(t)$	Conway notation
C_1:$(3_1,5_1,\ldots)$	$(1+t^C)/(1+t)$	C
C_1:$(4_1,6_1,\ldots)$	$\frac{C}{2}-1-(C-1)t+\left(\frac{C}{2}-1\right)t^2$	$(C-2)(2)$
C_2:$(5_2,7_2,\ldots)$	$\frac{C-1}{2}-(C-2)t+\frac{C-1}{2}t^2$	$(C-2)(2)$

towards the Flory coil conformation. $\overline{R_g(t)}$ denotes the average of $R_g(t)$ over many relaxation realizations and its behavior as a function of t is monitored. The chains eventually reach their final stages, the equilibrium state of the linear unknotted chain, within the course of our simulation. Also, all the relaxation processes can be well fitted into exponential curves. The nonequilibrium relaxation time τ is extracted from the data of $\overline{R_g(t)}$ by assuming that $\overline{[R_g(\infty)-R_g(t)]/[R_g(\infty)-R_g(0)]}$ decays as $\exp(-t/\tau)$. It is worth mentioning that Quake, in his work on the equilibrium relaxation behavior of knotted chains [8], found a long time mode for all the relaxation curves. He fitted the relaxation curves by the sum of two exponentials, with independent magnitudes and relaxation times. Our results on nonequilibrium relaxations do not show an obvious long time mode and no stretched exponential behavior is observed. Figure 3 shows the variation of τ versus p for various knots. τ for the trivial knot 0_1 is also shown for comparison. As shown, τ fluctuates up and down, although the overall trend shows an increase in τ with increasing p. This suggests that the local topological structure plays an equally important role in the relaxation dynamics of a cut knotted polymer as the degree of compactness does. After careful visual inspection of the knot diagrams, we find that these prime knots can be divided into groups, based on their topological similarity. These groups are $(3_1,5_1,\ldots)$, $(4_1,6_1,\ldots)$, $(5_2,7_2,\ldots)$, etc. (see Fig. 1 for these knot groups). It is somewhat surprising that 3_1 has a longer relaxation time than 4_1 and 6_1, despite its fewer crossings and a much smaller value of p. In the study of the equilibrium relaxation behavior of knotted polymers, Quake [8] also mentioned an obvious slow relaxation for 3_1 as compared to 4_1, 6_1, 8_1, 10_1 for some unknown reason. This can be easily interpreted from our classification, since 3_1 belongs to the group of longer relaxation. From Fig. 3 we can see that the group $(3_1,5_1,\ldots)$ has longer relaxation times than other groups for knots with the same N or p. This indicates that the $(3_1,5_1,\ldots)$ group has the strongest topological hindrance on the relaxation moves among the groups studied, which may be related geometrically to the fact that the knots in this group are $(2,C)$ tori (i.e., the knot can be placed on the surface of a torus). Thus the topological effects have much stronger influences on the relaxation dynamics (both equilibrium and nonequilibrium) than on the static properties. By analyzing the Alexander polynomials $[\Delta(t)]$ of these groups of knots, we find that the knots in each group have a similar form for their Alexander polynomials parametrized by the number of crossing C, as listed in Table I. Then from the form of these polynomial invariants, it is easy to see why the relaxation behavior is divided into groups; the local topology of a knot determines the relaxation and the similarity in the local topology is reflected in the same class of polynomial invariants. Furthermore, the group $(3_1,5_1,\ldots)$, which has a long τ, may also be associated with the observation that the degree of $\Delta(t)$ increases with C, while for the other two groups their $\Delta(t)$'s are always of degree 2. Such a classification of knots into these groups is further supported by the observation that the Conway notations [7] of the knots in the same group are parametrized in the same way (see Table I).

The relaxation time data of the $(3_1,5_1,\ldots)$ group smoothly increases as $\tau\sim p^{12/5}$ (upper solid curve in Fig. 3), while the $(5_2,7_2,\ldots)$ group deviates more significantly from this behavior, but appears to merge with the $\sim p^{12/5}$ behavior at large p (lower solid curve). It can be seen from Table I that the $\Delta(t)$'s of the latter two groups become asymptotically the same for $C\gg 1$ (i.e., large p). Thus we anticipate that for sufficiently large p, these two groups will have the same $\tau\sim p^{12/5}$ relaxation behavior. The local topological effects on the relaxation of these groups can also be understood in terms of their Conway notations. For the $(3_1,5_1,\ldots)$ group, the essential crossings form a braid topology (see Fig. 1) and the Conway notation is just a single integer denoting the number of crossings in the braid. For the other two groups, the first integer in the Conway notation is again the number of crossings $(C-2)$ in the braid structure, while the second integer is the number of crossings in the right part of the knot diagram, which is fixed to be two for these two groups. Thus it is easy to see that for large values of C (and hence p), the relaxation behavior will be dominated by the braid structure in these knots. Our data suggested that the $\tau\sim p^{12/5}$ behavior accounts very well for the relaxation of the ''pure braid'' structure in the $(3_1,5_1,\ldots)$ group. The other two groups appear to approach this predicted behavior for large values of p.

The idea of ‘‘creeping motion’’ of the polymer in an inflated tube is employed here to estimate the nonequilibrium relaxation time. When the chain is cut at $t=0$, the constraint of the ‘‘end-to-end’’ connection is relieved and the chain starts to relax. In good solvents, the chain would tend to expand out of its compact structure. However, the prohibition against chain crossing hinders the process. This effect is especially obvious in the relatively compact knot. Thus, the relaxation process can only proceed through a ‘‘diffusion along a tube’’ type of motion. However, unlike in standard reptation theory [15] in which cross-linked network or polymer melts are considered and the monomers move in a ‘‘tube’’ resulting from the obstacles produced by other chains, the topology of the surrounding did not change significantly in the intermediate time scales. In the present case, we find that the radius of gyration expands at the same rate as the end-to-end distance does. In other words, the diameter of the ‘‘tube’’ expands accordingly and is also much larger in the present case. Even so, we believe that for relatively complex knots, the creeping move along an inflated tube is the dominant part in the relaxation process. Employing the idea of a maximally inflated tube [11,12] of contour length L and cross-section diameter d, the average time τ, taken for the chain to creep out of the initial contour length L, can be evaluated as $\tau \sim L^2/D$. The diffusion coefficient D can be calculated as $D=k_B T/\mu_t$ where k_B is the Boltzmann constant and μ_t is the total friction coefficient. As we know, the friction coefficient for the chain in a tube of solvent is proportional to N, i.e., $N\xi$, where ξ is the monomer-solvent friction coefficient in the Rouse model [15]. However, an internal friction process is also involved as the chain varies its conformations during the relaxation process. For a linear polymer chain, the monomers tend to avoid each other in good solvents and the probability of two monomers in direct contact is small. However, for knotted polymers, monomers are in close contact because of the existence of crossings. After cutting the knots, monomers will slide onto each other and extra friction will occur during relaxation. The collision probability is greatly increased as the number of crossings increases. This monomer-monomer friction does not involve the solvent, but will be somewhat related to the viscosity of a fluid of monomers. We use an analog to electric resistance to estimate this internal friction and assume it to be proportional to the ratio of length to the cross-section area of the maximally inflated knot. Thus $\mu_t = N\xi + L\zeta$, where $\zeta \propto 1/d^2$. Following the idea on the construction of the maximally inflated tube, Grosberg *et al.* [11] obtained $L \sim R_g p^{2/3}$ and $d \sim R_g p^{-1/3} \sim N^{\nu} p^{-3/5}$. Thus $\mu_t = N\xi + \zeta_o N^{-\nu} p^{8/5}$ for some characteristic monomer-monomer friction ζ_o and hence $\tau \sim L^2/D \sim N^{2\nu} p^{4/5} [N\xi + N^{-\nu} p^{8/5} \zeta_o]$. For fixed p and $N \gg 1$, $\tau \sim N^{1+2\nu}$. For fixed N and $p \gg 1$, $\tau \sim p^{12/5}$. The relation $\tau \sim p^{12/5}$ gives a good description for our data in Fig. 3, especially for the braid structure in the $(2,C)$ tori group. We have also found [14] that the $\tau \sim N^{1+2\nu}$ relation is consistent with our simulation data for the 3_1, 4_1, and 5_1 knots.

The importance of the topological effect can be further verified from the outcome of a naive attempt to derive for the relation between τ and p in the following. If the knot has a greater value of p (i.e., is more compact), then simple calculations show that it has a larger free energy difference from the Flory free coil state, and hence the relaxation process should proceed faster. But this is contrary to what we find in simulations. This is due to the existence of the free energy barrier that arose from the topological effect and is not accounted for in the naive free energy difference approach. The system does not simply just relax downhill to the lower free energy Flory coil state, but has to overcome the barrier due to the topological constraint of entanglements. Thus for the study of dynamical properties of knots, the topological effect is a critical factor.

This research is supported by the National Council of Science of Taiwan under Grant No. NSC 87-2118-M-008-015. Computing time, provided by the Simulational Physics Laboratory, National Central University, is gratefully acknowledged.

[1] W. R. Bauer, F. H. C. Crick, and J. H. White, Sci. Am. **243**, 118 (1980).
[2] N. R. Cozzarelli, S. J. Spengler, and A. Stasiak, Cell **42**, 325 (1985).
[3] S. A. Wasserman and N. R. Cozzarelli, Science **232**, 951 (1986).
[4] V. F. R. Jones, Bull. Am. Math. Soc. **12**, 103 (1985).
[5] F. Y. Wu, Rev. Mod. Phys. **64**, 1099 (1992).
[6] L. H. Kauffman, *Knots and Physics*, 2nd ed. (World Scientific, Singapore, 1993).
[7] G. Burde and H. Zieschang, *Knots* (Walter de Gruyter, Berlin, 1985).
[8] S. R. Quake, Phys. Rev. Lett. **73**, 3317 (1994).
[9] Y.-J. Sheng, P.-Y. Lai, and H.-K. Tsao, Phys. Rev. E **56**, 1900 (1997).
[10] M. P. Allen and D. J. Tildesley, *Computer Simulations of Liquids* (Oxford University Press, New York, 1987).
[11] A. Yu. Grosberg, A. Feigel, and Y. Rabin, Phys. Rev. E **54**, 6618 (1996).
[12] V. Katritch, J. Bednar, D. Michoud, R. G. Scharein, J. Dubochet, and A. Stasiak, Nature (London) **384**, 142 (1996).
[13] V. Katritch, W. K. Olson, P. Pieranski, J. Dubochet, and A. Stasiak, Nature (London) **388**, 148 (1997).
[14] Y.-J. Sheng, P.-Y. Lai, and H.-K. Tsao (unpublished).
[15] M. Doi and S. F. Edwards, *The Theory of Polymer Dynamics* (Oxford University Press, Oxford, 1992).